TEST OF FUSION REACTOR MATERIALS WITH CYCLOTRONS AND PRESENTATION OF THE KARLSRUHE DUAL-BEAM FACILITY

by

A. Möslang, S. Cierjacks, and R. Lindau
Kernforschungszentrum Karlsruhe
Institut für Material- und Festkörperforschung II
Postfach 3640, D-7500 Karlsruhe
Federal Republic of Germany

ABSTRACT

A brief outline is given on the principal operating conditions of tokamak-type fusion plants and the consequences for fusion reactor materials development. For example, the loading of the first wall, the first solid barrier between the plasma and the outside of the reactor is, beside the plasma-surface interactions, a combined effect of oscillating temperature gradients, giving rise to thermal fatigue and damage due to high fluxes of ≤14 MeV DT fusion neutrons. In view of these severe loadings, resulting in a change of the mechanical properties, the present materials research programs need test facilities, where fusion-relevant conditions can be adjusted in macroscopic specimen.

Unfortunately, there are presently no intense sources of 14-MeV neutrons capable of providing sufficiently high fluxes over large volumes. Several attempts to overcome this difficulty by using other broad-spectrum neutron sources, based on various source reactions, are presented. The advantages and limitations in tailoring fusion-similar conditions at cyclotrons and other light-ion accelerators are outlined. Special emphasis is given to experimental facilities that can simulate certain aspects of radiation damage effects by charged-particle bombardment.

Finally, the Karlsruhe Dual-Beam Facility is presented, where α-particles from an isochronous cyclotron (104 MeV) and protons, variable in energy (15-42 MeV), are focused onto a common target. The advantages of this facility, which allows not only the simulation of fusion neutrons by the systematic variation of hydrogen, helium and damage production, but also reactor-relevant mechanical loadings in thick metal and ceramic specimen, are shown together with experimental results. This Dual-Beam Facility was developed within the European Fusion Technology Program.

1. INTRODUCTION

Research in the field of controlled thermonuclear fusion has been carried out for a few decades, with a lot of scientists and engineers are working in many countries to develop tokamak-type fusion devices as one of the most promising systems. These efforts have led to considerable progress over the past few years. The challenge of getting a positive energy balance in a fusion reactor and of establishing engineering feasibility are extremely high. However, the energy break-even or scientific feasibility demonstration is expected in the next few years with the reaction

$$D + T \rightarrow He\ (3.5\ MeV) + n\ (14.1\ MeV),$$

and will need to be followed by an intensive program of technological development.

Consequently, the next generation of fusion devices as they are discussed at present, i.e., the International Thermonuclear Experimental Reactor (ITER) or the Next European Torus (NET), have the objectives not only to show fusion energy production but also to demonstrate the feasibility of fusion from technological points of view. Fig. 1 shows the layout of such a device [1]. Any other

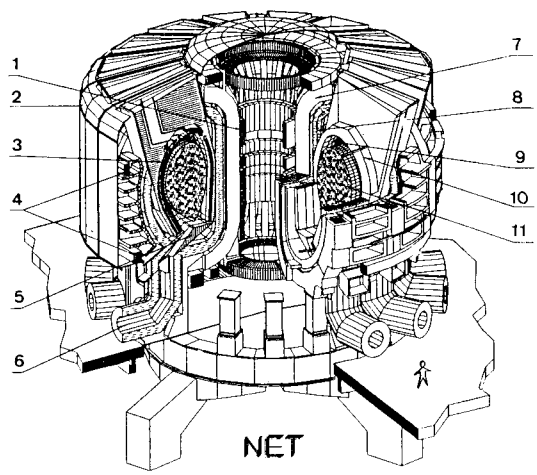

Fig. 1: General view of a fusion device (NET) showing the main components: 1. Inner poloidal coils 2. Cryostat 3.+9. First wall 4. Outer poloidal coils 5. Divertor plates 6. Plasma exhaust 7. Toroidal field coils 8. Shield 9. Blanket 11. Plasma.

tokamak reactor will have the same features, though details of the design may be different. The general perspectives of fusion are described in a number of books and reports, e.g. [2,3].

For the evaluation of structural materials the knowledge of their fusion-specific loading conditions is necessary. These materials can roughly be devided into two classes, the metallic and the non-metallic structural materials. Non-metallic materials are necessary mainly for insulators, radiofrequency and high frequency heatings, for diagnostic windows and neutral beam injectors. Because these parts show low thermal conductivity and much higher sensitivity to irradiation defects than metals, they have recently received substantial attention. Among the metallic materials, the plasma-facing components, namely the first wall and the divertor work under the most severe conditions. But also the complex structure of the tritium breeding blanket, which is an essential part for the concept of DT-devices, may be lifetime limited because of corrosion problems and high neutron irradiations. Several international conferences on fusion materials, e.g. [4] and workshops on microstructure evolution under fusion conditions, e.g. [5,6], show the efforts to gain a better understanding of the key scientific and technological problems in the field of fusion reactor materials.

In the following we will focus attention to the loading of first wall (FW) materials and on experimental devices which can help to adjust fusion similar conditions. The decision on the NET construction is planned [1] in 1993. In the meantime, an extensive database should be collected for other device concepts also as a basis for design solutions and feasible technologies.

2. FW LOADINGS IN FUSION DEVICES

2.1 Surface Loading by Plasma Particles

Fig. 2 shows schematically the loading of a first wall by plasma particles and fast fusion neutrons. Because of their short range high local concentrations of hydrogen isotopes and helium can be accumulated below the surface leading to surface bubbles and sputtering. In Fig. 3, which compares

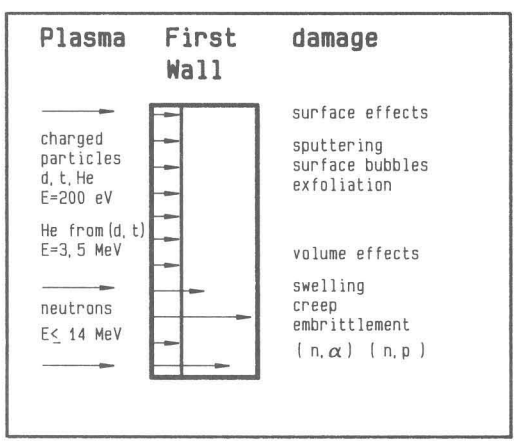

Fig. 2: Plasma particle and neutron-induced loading of a first wall (schematic).

an irradiated vanadium surface with an unirradiated one [7], these effects are clearly visible. However, the use of divertors drastically reduce the interaction of plasma particles with a first wall resulting in tolerable sputter rates. The thermal

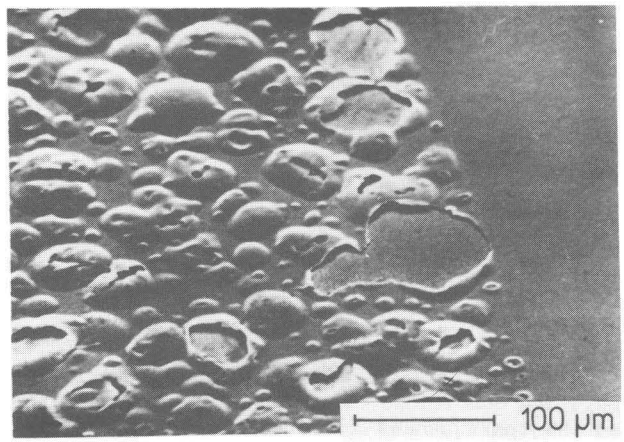

Fig. 3: SEM micrograph of vanadium after implantation with 240 keV He (625 °C) at a dose level of 2.4x10**17 cm**-2 showing a comparison between irradiated and unirradiated surface [7].

heat deposition connected to these plasma particles is about 15 W/cm**2.

2.2 Neutron Wall Loading

Displacement damage: The high energy fusion neutrons have mean free diffusion paths in the mm-range and can easily penetrate the first wall. During thermalisation they loose their energy either by elastic and/or inelastic scattering with the nuclei of the lattice atoms. Depending on the amount of energy transferred to one recoil nucleus (elastic interaction) single atoms can be displaced from their lattice sites or defect cascades varying in size and shape can be produced. This way the first wall suffers substantial irradiation damage like decrease of ductility, matrix hardening, embrittlement, swelling and radiation enhanced creep. Usually this damage is measured in "displacement per atom (dpa)" and can be calculated with well known methods (e.g. NRT-model [10-12]). As can be seen from Table I the defect rate under fusion conditions is 3x10**-7 dpa/s and a total damage of about 10 dpa will be accumulated.

Transmutation isotopes: The irradiation of 14 MeV neutrons is dominated by inelastic scattering. In addition to the displacement damage transmutation products like hydrogen isotopes and helium will be produced (Table I), which are typically 100 times larger than those of fission reactors [13]. In particular, the ratio He-dose/damage seems to play an important role due to the insolubility of helium precipitating in bubbles and at grain boundaries. Especially at temperatures above 500 °C and at He-contents above about hundred appm "high temperature helium embrittlement" is a well known effect. The amount of hydrogen produced in plasma-faced materials is about five times that of helium (Table I). The diffusivities, solubilities and permeabilities of hydrogen isotopes in unirra-

diated austenitic and ferritic steels are reasonably well established. In contrast to helium, hydrogen isotopes show orders of magnitude higher diffusivities [14] and the main fraction is believed to escape from the first wall again [15]. However, the hydrogen remaining in the precipitation rich matrix can contribute to embrittlement and crack propagation, at least at lower temperatures [16-19]. There is some evidence [20] that implanted helium together with irradiation defects

Table I. Typical NET first-wall operating conditions relevant for materials testing [1,8,9]

Fusion power	1100 MW
Mean neutron wall load	1 MW/m^2
Mean defect rate	3 $x10^{-7}$ dpa/s
Mean radiation damage	10 dpa
Sputtering erosion (steel)	0.2 mm/a
He/dpa (steel)	~10 appm He/dpa
H/dpa (steel)	~50 appm H/dpa
Pulse number	10^4 - 10^5
Pulse length	50 - 1000 s
Temperature (phase 1)	155 - 300 °C
(phase 2)	260 - 500 °C
Materials (steel)	Austenite 316L and Martensite DIN 1.4914

can act as effective hydrogen traps. Additional investigations under fusion typical conditions are necessary to confirm these effects.

The amount of produced transmutations is not only dependent on the chemical composition but also on the neutron energy varying between 14.1 MeV and thermal values. Thus, it is obvious that fusion neutrons introduce more severe demands on materials than fission neutrons.

2.3 Pulsed Load and Fatigue

A specific feature of tokamak fusion devices are the plasma burn and off-burn periods generating thermal cycling. Depending on the pulse length (≤1000 s), the operating conditions and the thermal conductivity of the first wall and the blanket, these oscillating temperature gradients will cause elastic or elasto-plastic reversed deformations giving rise to thermal fatigue which at present is considered as the main lifetime-limiting phenomenon. This fatigue problem is especially difficult for austenitic steels with their low thermal conductivity. Evaluations of the fatigue life have shown that in these alloys the first wall will be at the limit of operation.

Thermal fatigue is usually investigated by cyclic variation of an applied strain between a maximum (tensile) and a minimum (compressive) amplitude. During these strain-controlled low-cycle fatigue (LCF) tests the induced stresses are measured together with the number of cycles to failure. Both values characterize the fatigue properties unambigously and are an important basis for the layout of structural fusion materials.

3. FACILITIES FOR FUSION MATERIALS TESTING

3.1 General Aspects

With the continuous progress towards breakeven fusion facilities, more thought has recently been given to the material that will be used in power-producing fusion demonstration reactors. High fluxes of ≤ 14-MeV neutrons of the order of ≥ 1x10**14 n cm**-2 s**-1 in volumes of more than 20 dm**3 are requested for present materials research programs [21]. Materials must be tested with loadings similar to end-of-life conditions, because material properties are not only non-linear with neutron dose, but can also be non-monotonic. Thus displacements of ≥ 100 dpa (displacements per atom) and helium and proton productions of ≥ 1000 appm (atomic parts per million) must be achieved, before the first fusion demonstration reactor can be built. Fission reactors can produce the necessary neutron fluxes in large volumes, but cannot provide the required high neutron energies. Even in the core of fast reactors the Watt-like spectra drop off exponentially above about several 100 keV. Nevertheless, it has been useful to study irradiation phenomena like matrix hardening and embrittlement, which are determinated by the defect structure, in such reactors. While being able to produce the necessary displacements, fission reactor sources cannot match the proton and helium production to the displacement rate, nor to the realistic rate of other transmutation products.

3.2 Status of Neutron Sources

Unfortunately, there is presently not any neutron source capable of producing very large fluxes of 14-MeV neutrons over large volumes (up to many dm**3). The two available intense source reactions for production of monoenergetic 14-MeV neutrons are i) the T(d,n) reaction with ~200 keV deuterons incident on a tritium target and ii) the DT fusion reaction. Both reactions presently cannot provide the necessary neutron fluxes needed for bulk-effect radiation damage studies. For the T(d,n)-reaction, this has only an efficiency of ~ 8x10**-5 neutrons per deuteron and a high heat production of 2500 MeV per source neutron, deposited in the target. The most intense 14-MeV source at present, based on the T(d,n)-reaction, is the RTNS-II (Rotating Target Neutron Source) at Livermore [22] which is restricted to fluxes of less than 10**13 n cm**-2 s**-1 in small volumes of ~1 cm**3. In a recent concept study for a much more intense 14-MeV DT source at Karlsruhe, NERO [23], a total intensity of a few 10**15 n/s was anticipated, but the resulting fluxes would also not exceed ~2x10**13 n cm**-2 s**-1 in a volume of 500 cm**3. In contrast, the DT fusion reaction is much more favourable with its specific neutron production yield of ~ 1 neutron per fusion reaction and a heat deposition in the target of 3 MeV/n. But even in this case, very intense sources of this type cannot be realized except, for operating fusion reactors themselves. The most promising DT fusion engineering facility is presently the plasma-based source studied at Livermore, which promises an intense flux up to 5x10**18 n/cm**-2 s**-1 in a fully-ionized high-density tritium target [24].

Spallation sources: Sufficiently high fluxes of high-energy neutrons can, in principle be achieved with modern spallation neutron sources. These sources, which have been primarily built for

condensed-matter research in the thermal and epithermal neutron energy range, also provide outstanding high-energy neutron fluxes from the primary (unmoderated) target. This is due to the fact that spallation reactions with light ions (protons or deuterons) of ~1 GeV on heavy element targets provide 20-40 neutrons per incident particle with a modest heat deposition of 25 to 50 MeV/neutron. Presently operating spallation sources already provide total intensities of up to a few 10**16 high-energy neutrons per second [25], and there are already upgrading concepts for most of the existing sources which aim at 1 to 2 orders of magnitude higher source strengths. But even with the suggested upgradings of the present facilities the inherent potential of the spallation source concept is by far not exhausted. For energy applications (accelerator breeding) sources with more than ten times higher fluxes than that anticipated for the upgraded machines have already been studied for a long time. Neutron production from spallation reaction mainly proceeds through two types of reaction mechanisms, and provides broad continuous neutron spectra ranging from the keV- to the few-100-MeV region: In the first step, high-energy neutrons are produced by intranuclear cascade reactions which give strongly forward-peaked neutron spectra. In a second step, evaporation neutrons are emitted from highly excited compound nuclei, and their angular distribution in the laboratory system is almost isotropic. On this basis, the shape of neutron spectra from spallation sources is selectable to a certain extent by choosing a reasonable emission angle. For fusion materials applications, the most favourable neutron spectrum is at backward angles, where the high-energy tail of cascade neutrons is largely suppressed. Radiation damage studies with spallation neutron sources have been performed already at the Radiation Effect Facilities of IPNS at ANL and of MEIN at BNL [26,27].

But even for backward spectra, the problem with the remaining portion of very high-energy neutrons cannot be avoided in applications for fusion materials studies. This is mainly due to displacement damage effects: When a primary knock-on atom (PKA) has high kinetic energy, it can produce a cascade damage, which does not occur, when the energy transferred to the knock-on atoms is much lower. In the latter case, it typically produces only a single Frenkel pair. Thus a suitable use of spallation neutron sources for fusion radiation damage studies depends on a careful assessment of PKA spectra, and a comparison with those produced in future fusion reactors. Furthermore, it is important to study, whether realistic transmutation rates (primarily for the production of H and He atoms) can be suitably matched to the expected displacement rates, before their general usefulness can be judged.

Medium-energy light-ion sources: High-energy neutron production with medium-energy light-ion beams is also a very effective method for intense neutron production, which largely exceeds the present possibilities of T(d,n) reactions. In the range below 100 MeV, proton and deuteron beams are most efficient for neutron production due to their sufficiently long range in thick (totally absorbing) targets. Neutron production with these ions at an energy of less than ~50 Mev is largely governed by competition of atomic and nuclear interactions in the target. Above that energy, nuclear interactions predominate more and more, and ultimately show the spallation-type reaction mechanisms. For deuterons a favourable additional neutron-producing process is the break-up of the projectile in the Coulomb and the nuclear field of the target nucleus. This provides a strongly forward-peaked neutron spectrum with a broad maximum centered around about half of the incident deuteron energy. In contrast to spallation reactions, optimum intensity is achieved with light-element targets. With 35-MeV deuterons on thick lithium targets, specific neutron yields of 5x10**-2 n/d can be achieved. The corresponding heat deposition in the target is ~500 MeV/n. Neutron sources based on this reaction mechanism have been realized in many laboratories [28], mostly involving medium energy cyclotrons. Broad spectrum cw sources have been used extensively in the past for radiation damage studies. e.g. the AVF cyclotrons at Oak Ridge and at the University of California have been used for high intensity of ~ 5x10**12 n/s sr [25]. While this intensity was fully sufficient for the study of some basic properties of radiation damage, considerably higher neutron fluxes are needed for the study of radiation damage bulk effects.

Deuterium-lithium sources: Several studies of high-performance deuterium-lithium sources which involve deuteron linear accelerators [29-31] have been performed. An early design concept of this type was the Fusion Materials Irradiation Test Facility (FMIT) at Hanford [29], which was abandoned as a national US source several years ago. The FMIT concept has been recently revived by Lawrence et al. [31], who proposed, on the basis of recent accelerator achievements, an improved International Fusion Materials Irradiation Test Facility (IFMIF). For the IFMIF deuterium-lithium source the new driver is based on the idea of multiple accelerator modules, with each module consisting of two radiofrequency quadrupoles funneling 3 MeV cw deuteron beams into a 35-MeV drift-tube linac for a 250 mA average beam current. Such a source could provide ~ 3x10**14 fast neutrons per cm**-2 s**-1 in a volume of ~ 500 cm**3. But apart from the fact that this type of source does not yet exist, such a source would be rather expensive in capital investment and operation costs. In addition, the high-energy high-intensity neutron fluxes are only achieved at the expense of a large fraction of neutrons with energies above 14 MeV (up to 50 MeV). This causes major concern to materials scientists with respect to element transmutations, other than those produced by 14-MeV (and lower energy) neutrons. From a materials research point of view, this can disturb the real picture of radiation damage, and it is not yet very clear, how the additional effects from neutrons above 14 MeV can be separated from those really produced in future fusion reactors.

3.3 Simulation with Ion Beams

Since, as shown above, suitable neutron sources for fusion materials testing are presently not available (at least not for studies of bulk irradiation effects) tests of fusion reactor materials

must further widely rely on simulation experiments. Charged particles, which can produce cascade damage, are an universal tool to study various aspects of particle interactions with condensed matter. On the use of light ion beam facilities a large number of review articles have been written [32-35]. Basic physical phenomena like energy loss, stopping and range of particles [36-40], damage and cascade formation [41,42] are investigated and related to the microstructural evolution which causes changes in the macroscopic material properties [43].

Heavy ions: If the energy is high enough (≥40 MeV), a uniform damage region, some few µm below the surface, can be created [45]. Such irradiations are well-suited for transmission electron microscopic (TEM) investigations. However, the typ-

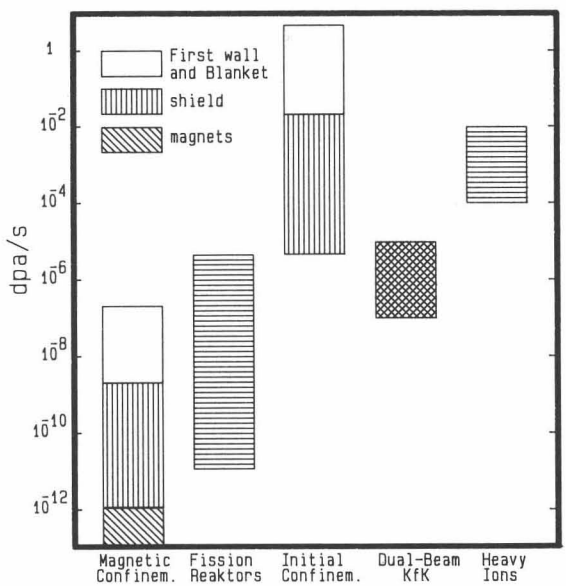

Fig. 4: Comparison of damage rates for different irradiation facilities [57]

ical damage rates between 10**-2 and 10**-4 dpa/s are orders of magnitude (Fig. 4) above fusion relevant values, and mechanical tests are not possible.

Light ions: An important advantage of light ions is their relatively large range that allows mechanical tests to be carried out during (in-beam tests) or after irradiation (post-irradiation tests). For example, a 100 µm steel foil, which is thick enough to perform creep or tensile experiments, can be penetrated by 6-MeV protons or 25-MeV α-particles. If their energy is high enough, even LCF specimen can be irradiated with a sufficiently constant damage depth profile. In addition irradiation-induced nucleation processes are controlled at defect rates typical for light ion irradiations (≤10**-4 dpa/s) by the material specific sink properties, and not by the defect rate itself. Thus, the comparison of experimental data between light ions and neutrons should lead to similar results. The displacement cross section which adjusts cascade sizes and densities is similar for 14 MeV neutrons and medium energy (15-25 MeV) protons and deuterons [44]. A disadvantage of light ion bombardment is, that it produces a larger number of single defects than high energy 14 MeV neutrons, because of the Coulomb scattering of the ions on the lattice atoms. The influence of the cascade to single-defect ratio on the resulting defect structures is presently discussed and needs further theoretical and experimental investigations. Another disadvantage is the operating cost of cyclotrons which restricts the integral damage level of irradiated specimen usually to about 1 dpa. Finally, it is possible with light ion irradiations to combine relevant damage generations and gas production. Implantation techniques with suitable degrader systems allow the adjustment of all fusion relevant He/dpa and H/dpa ratios.

A broad-scale survey of light-ion beam facilities has been recently given by Shiraishi et al. [44] (compare Tables 1,2 of this author). Recent experimental investigations of fusion relevant materials are focused mainly on irradiation creep, e.g. [45], creep rupture e.g. [46] and tensile properties, e.g. [47] as well as on helium TEM-observations contributing to the field helium-bubble nucleation and evolution [48]. Almost all experiments with cyclotrons were carried out with ions in the energy range between 6-50 MeV, and a few with 500-800 MeV protons [49-51]. These are very useful to study the influence of largely different ratios of single to cascade defect damages which vary largely for different high-energy particle irradiations.

3.4 Required Technology

The most important basis for the irradiation of specimen which could be mechanically tested is temperature and beam stability. This means that
- beam current fluctuations
- shifts of the beam position and
- changes of beam density profiles

should be avoided during specimen irradiation. Particularly beam current fluctuations within the time constant of the specimen cooling device are damaging to the temperature stability. Temperature is one of the most important parameters which control irradiation - induced defect migration and nucleation. For example, quick current changes of 8-10% cause short-time temperature shifts of typically 15% in specimen irradiated in vacuum. Thus the scatter band in mechanical experiments is usually enlarged and a meaningful microstructure analysis is almost impossible. Another parameter, which is sensitively correlated with the beam current is the damage and implantation rate. At least in uni-axial in-beam creep experiments, where a constant stress is applied to the specimen during irradiation, the creep rate (time dependent increase of the strain) is controlled by particle flux and temperature. Consequently, temperature variations of less than a few K are strongly desirable in in-beam creep or in-beam LCF experiments. For the compensation of the beam heating, cooling and/or heating devices are necessary. Usually inductance coils or direct electric current heating systems are used.

Whereas nuclear physics often requires high luminosity with focused beams, applications for material development need homogeneous beam densi-

ties within the irradiated specimen surface. This beam uniformity can easily be reached in "small sized" gauge areas of 8 mm x 2 mm, which are typical for some tensile and creep specimen, by defocussing the beam with magnets and degrader systems. However, specimen surfaces larger in size should be homogeneously irradiated with the use of special scanning magnets in order to take advantage of the beam current (see below).

Finally, suitable degrader systems are necessary to achieve a homogeneous depth distribution of implanted particles.

4. THE KfK DUAL-BEAM FACILITY

The Dual-Beam Facility of KfK, where alpha-particles (104 MeV) and protons (15-40 MeV) are focused onto a common target, was developed as a research tool for materials testing within the European Fusion Technology Program. This dual beam technique allows the simulation of fusion neutrons by the systematic variation of hydrogen, helium and damage production in thick metal and ceramic specimen as well as tokamak-relevant thermal cycling and mechanical loadings like low cycle fatigue in proposed first wall materials.

Even though all the previously performed investigations with light ion beams have considerably furthered our present understanding of irradiation damage and the relation between tensile or creep properties and microstructure, there are, to our knowledge, no other facilities which can combine proton and helium beams of sufficiantly high energy with low cycle fatigue experiments. Therefore, this facility allows for the first time to study simulation experiments on macroscopic specimen with two cyclotrons running independently of each other [52].

4.1 Range of Application

While alpha-particles are homogeneously implanted usually during dual-beam irradiations, the protons penetrate the specimen to adjust the fusion relevant or any other He-dose/damage ratio. The specimen geometry allows cyclic stress-strain loadings after and during irradiations. The combination of both beams together with suitable degrader systems, X-Y-scanning magnets and a powerful He-gas cooling device allows a large variability of the irradiation conditions:

- hydrogen and helium implantations can be independently adjusted up to several 1000 appm/week in thick specimen
- any implantation depth profiles are possible
- implantation range in steel: H 2.9 mm
  He 1.3 mm
- He-dose/damage ratios: 10-200 appm He/dpa in LCF specimens
  10-1900 appm He/dpa in tensile specimens
- systematic investigations of H and He effects allows the comparison of data between different cyclotron irradiations
- high flexibility in the choice of experimental parameters
  - irradiation temperature 100-720° C
  - damage rates (Fig. 4) 1-50x10**-7 dpa/s
  - beam cycling experiments
  - temperature cycling experiments up to about 5 K/s
- fatigue experiments are done by a computer controlled endurance machine operating in the stress or strain controlled mode. All fusion typical mechanical loadings can be adjusted.

It is presently believed that the He-dose to damage ratio is of particular importance. Fig. 5 shows a comparison of different topical facilities relating to the production of damage and helium in a martensitic steel. It is obvious that the helium production in fast breeder reactors (e.g. in KNK II) is typcially an order of magnitude too low, whereas the dual-beam facility allows systematic investigations of that ratio by deliberately injecting helium.

It is desirable in simulation experiments to ensure controlled irradiation parameters (e.g. temperature, damage and implantation profiles) at high beam currents in order to make efficient use of the irradiation time. Since the implantation rate decreases with increasing thickness, the geometry of specimen must be reduced down to a size which just ensures macroscopic material behaviour. Consequently, the specimen thickness should not fall below 100 µm in tensile specimen and 300 µm in fatigue specimen. On the basis of these requirements the specimen geometries in Fig. 6 were developed. Whereas this hollow LCF specimen ("H-GRIM" geometry) is suitable for many applications, it has to be replaced in future in-beam LCF experiments for various reasons. The necessity to develop a new specimen geometry, follows from the knowledge that cylindrical specimen had to be rotated at great expense during the in-beam LCF

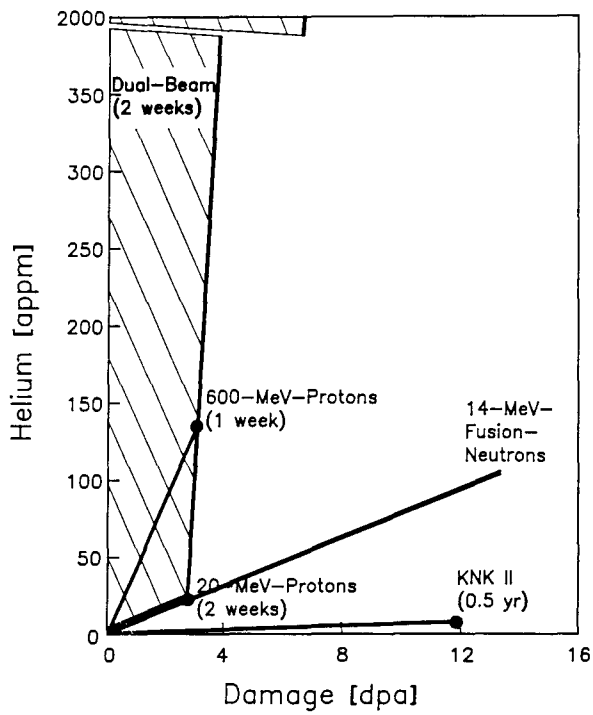

Fig. 5: Comparison of different irradiation facilities concerning the damage and helium production in ferritic steels.

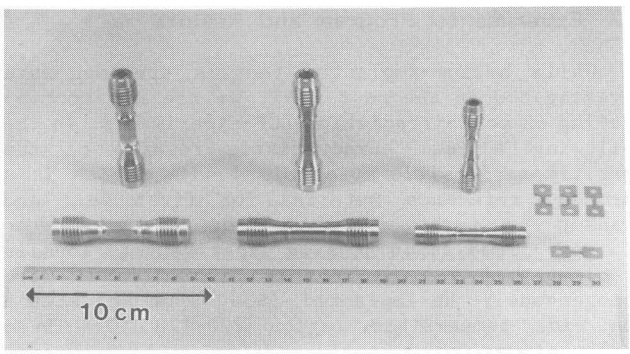

Fig. 6: Specimen used at the Dual-Beam Facility. Three different hollow fatigue specimen (left) and a tensile specimen (right).

experiment in order to achieve homogeneous temperature and irradiation conditions. The specimen devised for this application has a square cross section and a constant wall thickness of 0.4 mm within the irradiated gauge length. Extensive experimental as well as theoretical investigations have shown that with this type of specimen (Fig. 6 left side) the generation of material specific fatigue properties is easily possible.

4.2 Irradiation Facility and Stage of Development

The Karlsruhe Cyclotron Laboratory is operating two cyclotrons which are mainly used (Fig. 7) for research in nuclear physcis (KIZ), for medical isotope production, for industrial applications [53] and for the irradiation of materials under fusion similar conditions (Dual-Beam Facility).

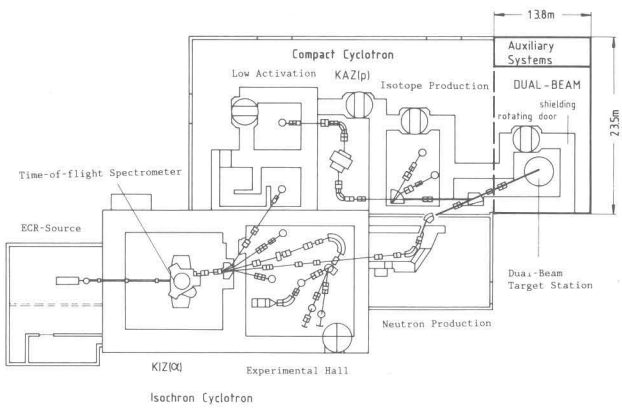

Fig. 7: The Karlsruhe Cyclotron Facilities.

To accomodate this facility it was necessary to extend the experimental hall and the existing beam lines by roughly 20 m. The angle between the two beams is only 10 degrees which leads to a fair coincidence across the specimen volume. The magnets and several beam diagnostic instruments are standardisized components generally used at the KfK cyclotron beam-line systems. The availability of the two beams for dual-beam experiments is presently about 1100 hours/year. The particle properties of the Dual Beam Facility are given in Table II and a front view of the Dual-Beam Facility with the diagnostic chamber (inside left), the experimental chamber (left side) and the beam lines (inside right) is shown in Fig. 8.

Table II. Particle properties of the KfK Dual-Beam Facility

Quantity	Isochronous Cyclotron (KIZ)	Compact Cyclotron (KAZ)	
Particle	α-particles	Protons	
Ion energy	104 MeV	15 - 42 MeV	
Beam current	10 μA	100 μA	
Beam spot	~ 1 cm^2	~ 1 cm^2	
Damage rate at the surface (dpa μA^{-1} cm^{-2})	1.1×10^{-7}	1.5×10^{-8}	(45 MeV)
		2.5×10^{-8}	(26 MeV)
Range in steel [39,54]	1.3 cm	3.5 cm	(45 MeV)
		1.3 cm	(26 MeV)

Target testing: A complex heating and cooling system was built to guarantee a homogeneous temperature profile at the specimen under different

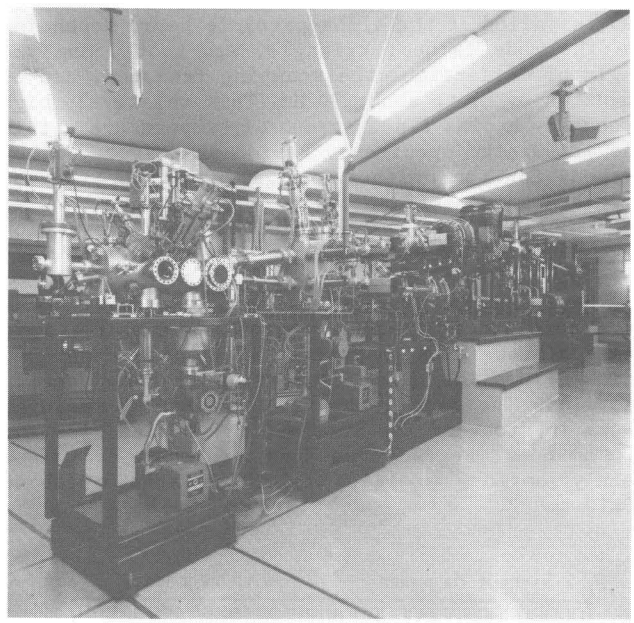

Fig. 8: Front view of the Karlsruhe Dual-Beam Facility with the experimental chamber, the diagnostic chamber and the α-particle and proton beam lines (from left to right).

irradiation conditions. For removing the irradiation induced heat deposition in tubular specimen a He-gas cooling loop operating at 2.5 bar with gas velocities near sound velocity was built. With this method about 350 W can be drawn off from the gauge volume at irradiation temperatures between 200 and 700 °C. The post-irradiation tests can be carried out with an endurance machine equipped with a high vacuum (1x10**-7 mbar). and a high temperature (1500 °C) furnace.

Data aquisition and process control: The experiment can be completely operated in manual as well as in remote mode. All signals coming from or going to the experiment are monitored by a real-time processing computer. The communication between the processor and the computer is maintained by structured program techniques using pyramidal structure. The supervising task controls the pro-

cess by a set of values predetermined by the experimentor or interactively changed by the operator during the process. The data are saved in structured files by the process computer and then periodically transferred to a central computer via a local network.

Implantation and damage profiles: Particle implantations are performed with sophisticated degrader systems [55] consisting of two water cooled microprocessor-controlled graphite wedges mooving quickly back and forth between two fixed positions. The angle straggling of the particles passing the degrader is taken into account by the velocity of the two wedges, which varies with the implantation depth. In this way even thick specimen can be implanted homogeneously without any concentration gradients. Because of the relatively high particle energies the damage gradient between the front and the back side of the specimen is sufficiently small. In order to achieve a homogeneous beam density profile also, a X-Y-scanning magnet was installed at the alpha-particle beam. Depending on the mode (sinus, triangle, saw-tooth) and the angle of deflection, the scanning frequency can be adjusted by up to about 30 Hz. This relatively high frequency avoids fluctuations of temperature within the irradiated specimen. Beside that system other methods for the uniform charged particle irradiation are known [56]. Non-linear optics can be used to transform a large fraction of particles which have Gaussian-like areal distribution into a uniform one.

Beam density profile monitor: In order to measure absolute beam density profiles within a wide range of densities, a monitor system was developed which allows the quick generation of beam density profiles. The density profiles in Fig. 9 measured 10 cm in front of the specimen are typical for the proton beam. Degrader passing protons lead to a fairly uniform profile within an area of about 10x10 cm**2.

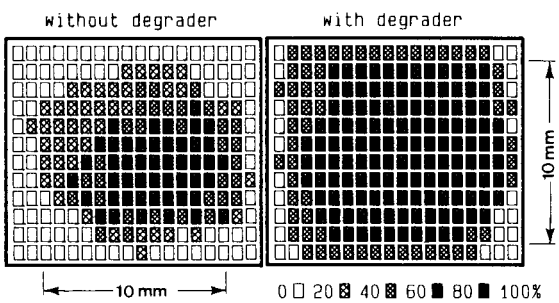

Fig. 9: Beam density profiles of the proton beam (30 MeV, 20 µA). measured with a newly developed profile monitor. Protons passing the degrader cause a fairly uniform profile with 10x10 mm**2.

Experimental chamber: To reduce the activity associated with high current irradiation all collimators are made of graphite, and the experimental chamber, formerly made of stainless steel was replaced by an aluminum one. Because of that the contact dose at the chamber surface dropped nearly two orders of magnitude.

4.3 Experimental Program and Results

While helium-implanted tensile specimen were investigated in the past [59], we are now concentrating on post-irradiation LCF-experiments. In the following a few characteristic results of the ferritic/martensitic steel DIN 1.4914, which is a European reference material for first wall and blanket structures, are presented.

Post-irradiation tensile experiments: Tensile specimen with a gauge size of 7x2x0.2 mm**3 were homogeneously He-implanted (≤340 appm He) within the wide temperature region 220-720 °C. These implantations were performed at a high He/dpa ratio. However, the damage rate was very similar to that predicted for NET, being in the range of 3x10**-7 dpa/s. After irradiation tensile tests were conducted mainly at temperatures equal to the irradiation temperature in a vacuum furnace. Fig. 10 shows the irradiation induced changes in the yield strength in comparison with neutron irradiated specimens. Obviously the main hardening is induced by displacement damage, which in the neutron irradiated specimen is about two orders of

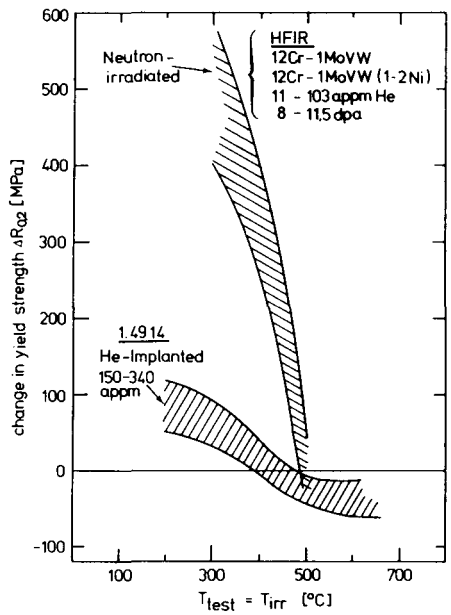

Fig. 10: Change in yield strength in 12% Cr-steels induced by helium implantation and neutron irradiation (HFIR) [57].

magnitude higher than in the He-implanted ones. An interesting feature is the hardening at temperatures below 400 °C and the softening above 450 °C. The underlying phenomena were analysed and the irradiation-induced change in yield strength can be understood quantitatively.

Besides mechanical experiments the knowledge of the microstructure before and after mechanical tests of irradiated specimen is inevitable, not only for the understanding of irradiation enhanced diffusion and solute segregation, but also for reliable lifetime predictions of helium containing components. The transmission electron microscopic (TEM) micrographs show very small defect clusters

("black dots") at 220 °C and a temperature dependent He-bubble evolution between 300 and 720 °C. Above 550 °C all bubbles are pinned at dislocations (Fig. 11), grain and lath boundaries or at the surface of precipitates. The helium induced swelling remains at all irradiation conditions substantialy below the swelling found in simultaneously He-implanted control samples of stainless steel 316L.

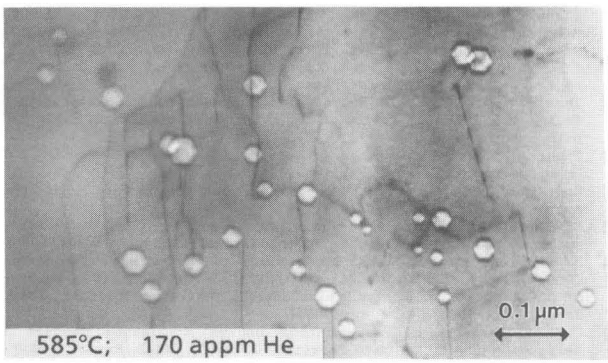

Fig. 11: TEM-micrograph showing He-bubbles pinned at dislocations in He-implanted and tensile-tested steel DIN 1.4914 [58].

Post-irradiation fatigue experiments: To investigate the effect of helium and damage on the low cycle fatigue behaviour at different temperatures, LCF specimens (H-GRIM geometry) made of steel DIN 1.4914 were irradiated between 300 and 600 °C with helium contents up to 1.2 dpa and damage levels up to 1.2 dpa. The irradiations were performed in vacuum using both beams simultaneously. The He-implantation rate varied between 0.1 and 2 appm He/h whereas the damage rate was fixed to about 0.01 dpa/s. After irradiation the specimens were low cycle fatigue tested and stress-strain diagrams were accumulated. In specimen with 200 appm He and 1.2 dpa the stress amplitude is increased at 300 °C by 11% whereas it is slightly decreased by only 1% at 600 °C (Fig. 12). At 450 °C the stress amplitude remains unaffected by He-

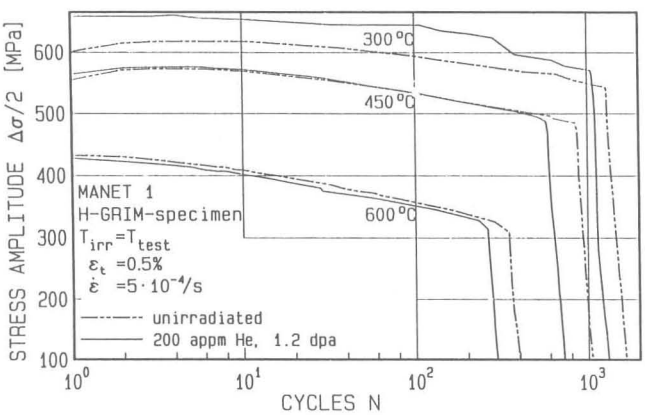

Fig. 12: Evolution of the stress amplitude during strain-controlled low-cycle fatigue testing in unirradiated and dual-beam irradiated fatigue specimen.

implantation. This behaviour corresponds with tensile tests under similar conditions, as shown above. Under all irradiation conditions only small changes in the number of cycles to fracture, N(f), were found. Helium contents between 65 and 200 appm tend to decrease N(f) up to 20%. Such small differences can be established because of specimen geometry which allows the determination of N(f) within 8-10%

Fractographic SEM observations (Fig. 13) following the fatigue tests show crack initiation at large precipitates and crack propagation perpendicular to the applied uni-axial stress along fatigue striations. These striations also show that the main crack moves within about 200 cycles through the wall.

The results confirm the general consensus of published data, that martensitic/ferritic steels like 1.4914 are highly resistant to irradiation induced helium embrittlement, even at much higher temperatures than those for a first wall and it is an encouraging result that the injection of helium does not significantly affect their fatigue properties.

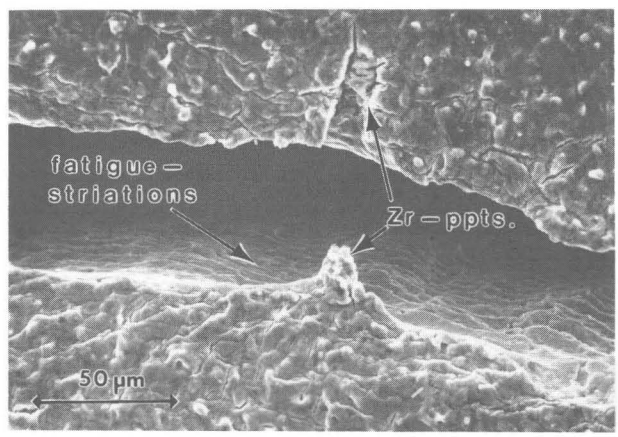

Fig. 13: SEM fractograph of fatigue tested martensitic 1.4914 specimen (T(test) = 450 °C in air, $\Delta\varepsilon_t$ = 0.6%)

5. CONCLUSION AND ACKNOWLEDGMENT

In conclusion, we have shown that light-ion irradiation reveals a unique feature in its possibilities for independently varying nuclear, mechanical and thermal parameters at the same time, especially when a cyclotron-based dual-beam technique is applied.

The authors wish to thank Dr. M. Rafat for providing computer-aided beam-density plots.

References

[1] R. Toschi et al., Next European Torus, Objectives, General Requirements, and Parameter Choices", Fusion Technology, Vol.14, 22 (1988).
[2] W. Haefele et al., "Fusion and Fast Breeder Reactors", RR-77-8, International Institute for Applied Systems Analysis, Laxenburg, Austria (July 1977).
[3] P. Holdren et al., "Report on the Senior Comittee on Environmental, Safety, and Economic Aspects of Magnetic Fusion Energy", UCRL-53766, Lawrence Livermore National Laboratory Report (1987).
[4] Proceedings of the 3rd Int. Conf. on Fusion Reactor Materials, (ICFRM-3), J. Nucl. Mater. Vol. 155-157 (1989).

[5] "The Relation between Mechanical Properties and Microstructure under Fusion Conditions", Ebeltoft 1985, Rad. Effects,101 Vol. 101, No 1-4 (1987).
[6] "The Effects of Recoil Energy Spectrum and Nuclear Transmutations on the Evolution of the Microstructure", Lugano, Switzerland, to be published in Rad. Effects (1989).
[7] D. Kaletta, "The Influence of Temperature on the Blister Behavior of V and Binary V-Ti-Alloys During 200 and 2000 keV He-Irradiation J. Nucl. Mater. Vol. 63, 347 (1976).
[8] R. Toschi, The NET Team (MPI for Plasmaphysics, Garching, W. Germany), CCFP and IN Reports, CCFP36/8 and IN 87-13 (1989).
[9] The NET team, "NET Status Report" (MPI for Plasmaphysics, Garching, W. Germany) (1985).
[10] J.M. Torrens and M.T. Robinson, "Radiation Induced Voids in Metals", USAEC Report, CONF-710601, p. 739 (1971).
[11] M.J. Norget et al., "A Proposed Method for Estimating the Number of Atomic Displacements in Irradiated Metals", AERE Technical Report, AERE/TP 494 (1972).
[12] R. Anderson and J. Adamson, "The Definition, Calculation, and Storage of Displacement Damage Dose Data", UK Atomic Energy Agency Report, UKAEA ND-M-3736(D) (1987).
[13] F.M. Mann, DAFS Quart. Prog. Report, DOE/ER-0046/24 p. 10, (1985).
[14] G. Alefeld and J. Voelkl, "Hydrogen in Metals I-II", Topics in Applied Physics, Vol. 28, Springer Verlag (1978).
[15] G. Gervasini and F. Reiter, "Tritium-Material Interaction in Various First Wall Materials", J. Nuclear Mater., Vol. 155-157, 754 (1988).
[16] G.F. Rodkey and R.H. Jones, "Effect of Internal Hydrogen on the Fatigue Crack Growth of a 12% Cr-steel", J. Nucl. Mater., Vol. 155-157, 760 (1988).
[17] S.P. Lynch, "A Fractographic Study of Gaseous H-Embrittlement and Liquid Metal Embrittlement in a Tempered Martensitic Steel", Acta Metall., Vol. 32, 79 (1984).
[18] J. Kameda, "Equilibrium and Growth Characteristics of Hydrogen-Induced Intergranular Cracking in Phosphorus-Doped and High-Purity Steels", Acta Metall., Vol. 34, 1721 (1986).
[19] T.P. Perng and C.J. Altstetter, "Effects of Deformation on Hydrogen Permeation in Austenitic Stainless Steels", Acta Metall., Vol. 34, 1771 (1986).
[20] D.R. Harries, "The Materials Requirements for NET", Radiation Effects, Vol. 100, Nos.1-4, 3 (1987).
[21] K. Ehrlich, "Requirements of Neutron Sources for Fusion Materials Testing", presented at the IEA Workshop on an International Fusion Materials Irradiation Facility (IFMIF), San Diego, USA, February 14-17, 1989.
[22] D.W. Heikkinen and C.M. Logon, "Recent Progress at RTNS-II", Nucl. Instrum. Meth. B10/11, 835 (1985).
[23] H.G. Dittrich et al., "Vorschlag für eine Neutronenquelle mit rotierendem Feststofftarget NERO", KfK-Report, KfK-3587, Sept. 1983.
[24] F.H. Coensgen et al., "A High-Performance Beam-Plasma Neutron Source for Fusion Materials Development", presented at the IEA Workshop on an International Fusion Materials Irradiation Facility (IFMIF), San Diego, USA, February 14-17, 1989.
[25] S. Cierjacks and A.B. Smith, "Neutron Sources: Present Practice and Future Potential", in Proc. of the International Conference on Nuclear Data for Science and Technology, Mito, Japan, May 30 - June 3, 1988.
[26] R. Birtcher et al., "Measurement of Neutron Spectra and Fluxes at the IPNS Radiation Effects Facility", in Proc. of the 6th Meeting of the Int. Coll. on Advanced Neutron Sources, 1983, p.407.
[27] T. E. Ward et al., "Radiation Effects Facility at the BNL 200 MeV Proton Linac", to be published in Nucl. Sci. Eng. (1989).
[28] M.A. Lone and C.B. Bigham, "Intense Deuteron and Proton Induced CW Sources", in Neutron Sources for Applications and Basic Nuclear Research, ed. S. Cierjacks, Pergamon Press, Oxford, p.133, (1983).
[29] A.L. Trego et al., "A Facility for Fusion Materials Qualification", Nuclear Technology/Fusion, Vol. 4(2) Part 2, 695 (1983).
[30] M. Mizumoto, "On the Concept of an Energy Selective Neutron Source for Materials Irradiation Studies", presented at the IEA Workshop on an International Fusion Materials Irradiation Facility (IFMIF), San Diego, USA, February 14-17, 1989.
[31] G.P. Lawrence al., "High-Performance Deuterium-Lithium Neutron Source for Fusion Materials and Technology Testing", presented at the IEA Workshop on an International Fusion Materials Irradiation Facility (IFMIF), San Diego, USA, February 14-17, 1989.
[32] D. Kaletta, "Light Element Implantations in Metals", Radiation Effects, Vol. 47, 237 (1980).
[33] H. Ullmaier et al., "Helium in Fusion Materials: High Temperature Embrittlement", J. Nuclear Materials, Vol. 133/134, (1985).
[34] H.Schröder et al., "Helium Effects on the Creep and Fatigue Resistance of Austenitic Steels at High Temperatures", Nucl. Eng. Design/Fusion, Vol. 2, 65 (1985).
[35] A.M. Omar et al., " Calculations of the Scattering and Radiation Damage Parameters for 14 MeV Neutrons and 10-20 MeV Protons on Fe, Ni, Cu, Zr, Nb and Au", J. Nuclear Mater., Vol. 64, 121 (1977).
[36] J.F. Ziegler, Handbook of Stopping Cross Sections for Energetic Ions in All Elements, ed. J. F. Ziegler, Pergamon Press, (1980).
[37] U. Littmark and J.F. Ziegler, Handbook of Range Distributions for Energetic Ions in All Elements, ed. J.F. Ziegler, Pergamon Press (1980).
[38] J.P. Biersack, "Basic Physical Aspects of High-Energy Implantation", Nucl. Instrum. Meth. Phys. Res., Vol. B35, 205 (1988).
[39] J.F. Ziegler et al., "The Stopping and Range of Ions in Solids", ed. J.F. Ziegler, Pergamon Press, (1985).
[40] Shang-chih P. Chou, "A Monte Carlo Approach to Ion Transport in Solids and its Application to Bulk and Surface Damage Analysis", UCLA Report, UCLA-ENG-8613, (1985).
[41] Physics of Radiation Damage in Metals, eds. R.A. Johnson and A.N. Orlov, Elsevier Science Publishers (1986).
[42] Radiation Damage in Metals, eds. F.A. Garner and S.D. Harkness, American Society for Metals (1976).
[43] Effects of Radiation on Materials, eds. F.A. Garner and J.S. Perrin, American Society for Testing and Materials (1985).
[44] H. Shiraizi et. al., " An Application of Cyclotrons to Radiation Damage Study for Fusion Reactor Materials Development", in Proc. of the 11th Int. Conf. on Cyclotrons and their Applications, Tokyo, Japan, Oct. 13-17, p. 571 (1986).
[45] G.P. Walters et al., "Radiation Damage Simulation Studies of Selected Austenitic and Ferritic Alloys", AERE Report, AERE-R 12620, (1987).
[46] P. Jung and N.M. Afify, "Creep of DIN 1.4914 Martensitic Stainless Steel under Proton Irradiation", J. Nucl. Mater., Vol. 155-157, 1019 (1988).
[47] U. Stamm and H. Schroeder, "The Influence of He on the High Temperature Mechanical Properties of DIN 1.4914 Martensitic Steel", J. Nucl. Mater., Vol. 155-157, 1059 (1988).
[48] H. Schroeder, "High Temperature He-Embrittlement in Austenitic Stainless Steels - Correlation Between Microstructure and Mechanical Properties", J. Nucl. Mater., Vol. 155-157, 1032 (1988).
[49] M. Victoria et al., "Nucleation and Growth of Precipitates and He-Bubbles in High Purity Al-Mg-Si-Alloy Irradiated with 600 MeV Protons", J. Nucl. Mater., Vol. 155-157, 1075 (1988).
[50] B.N. Singh et al., "Nucleation of the Bubbles on Dislocations, Dislocation Networks and Dislocations in Grain Boundaries During 600 MeV Proton Irradiation of Aluminum", J. Nucl. Mater., Vol. 125, 287 (1984).
[51] D.J. Farnum et al., "Effects of Radiation on Metals", Radiation Effects, Vol. 97, 42 (1986).
[52] D. Kaletta, "The High Energy Dual Beam Technique", J. Nucl Mater., Vol. 133/134, 878 (1985).
[53] V. Bechthold et al., "Industrial Applications of the Karlsruhe Compact Cyclotron", in Proc. 11th Int. Conf. on Cyclotrons and their Applications, Tokyo, Japan, Oct. 13-17, p. 593 (1986).
[54] J.F. Janny, " Calculations of Energy Loss, Range, Pathlength, Straggling, Multiple Scattering, and the Probability of Inelastic Nucl. Collisions for 0.1 to 1000 MeV Protons", Technical Report, AFWL-TR-65-150, (1966).
[55] A. Moeslang and D. Kaletta, Patent DE-OS 37 05 295 (1988).
[56] E. Kashy and B. Sherrill, "A Method for the Uniform Charged Particle Irradiation of Large Targets", Nucl. Instrum. Meth. Phys. Res., Vol. B26, 610 (1987).
[57] G.L. Kulcinski and M.E. Sawan, "Differences Between Neutron Damage in Inertial and Magnetic Confinement Fusion Materials Test Facilities", Report, UWFDM-607 (1984).
[58] R.L. Klueh and J.M. Vitek, "Postirradiation Tensile Behavior of Ni-Doped Ferritic Steels", J. Nucl. Mater., Vol. 150, 272 (1987).
[59] A. Möslang and D. Preininger, "Effect of He-Implantation on the Mechanical Properties and the Microstructure of the Martensitic 12% Cr-Steel 1.4914", J. Nucl. Mater., Vol. 155-157, 1068 (1988).